Peer-reviewed version available at Metals 2019, 9, 93; doi:10.3390/met9010093

Structure of solidified films of $CaO-SiO_2-Na_2O$ based low-fluorine mold flux

Jianhua Zeng[1], Xiao Long[2], Xinchen You[1], Min Li[1], Qiangqiang Wang[1], Shengping He[1*]

1. College of Materials Science and Engineering, Chongqing University, Chongqing, 400044, China.

2. Department of Materials and Metallurgical Engineering, Guizhou Institute of Technology, No.1 Caiguan Road, Guiyang, 550003, China.

E-mail: heshp@cqu.edu.cn

Keywords: mold flux, low fluorine, internal crack, surface roughness, slag film

Abstract: As an essential synthetic material used in continuous casting of steels, mold fluxes improve the surface quality of steel slabs. In this study, a $CaO-SiO_2-Na_2O$ based low-fluorine mold flux was solidified by an improved water-cooled copper probe with different temperatures of molten flux and different probe immersion times. The heat flux through solid films and the film structures were calculated and inspected, respectively. The results indicate: large internal cracks (formed in the glassy layer of films during solidification) were observed, the formation and evolution of those cracks contributed to the the unstable heat flux density. The roughness of the surface in contacted with the water-cooled copper probe formed as films were still glassy and the roughness have no causal relationship with crystallization or devitrification. Combeite with columnar and faceted dendritic shapes is the main crystal in the film.

1. Introduction

In the continuous casting of steels, mold fluxes control the heat flux from steel shells to the mold[1-3] by forming a solid slag film. For medium-carbon steels, large volume shrinkages caused by peritectic transition (delta ferrite to austenite) at meniscus make some steels quite crack-sensitive[4,5]. Thus, slow and uniform cooling are required to prevent the formation of longitudinal cracks on slab surfaces. The usual method to solve this problem is using mold fluxes to lower the heat flux from initial steel shells to the mold near meniscus. Conventional

Peer-reviewed version available at Metals 2019, 9, 93; doi:10.3390/met9010093

mold fluxes for peritectic steels usually have high-fluorine contents and high basicites (binary basicity from 1.2 to 1.5, $CaO-SiO_2-CaF_2$ based slags). As an important element in fusion agents (such as NaF, CaF_2 etc.), fluorine simplifies the microstructure of molten fluxes, decreases its high-temperature viscosities, and promotes the formation of cuspidine ($3CaO.2SiO_2.CaF_2$) in solid slag films[6-8]. Based on previous approaches[9,10], the precipitation of cuspidine in slag films is widely considered as a major contribution of high-basicity mold fluxes to decrease the heat flux. Therefore, fluorine is considered as a significant component in mold fluxes for peritectic steels, and which usually up to 10 mass percentage or more. However, fluorine-containing gases (mostly reported as NaF and SiF_4) evaporate from molten fluxes at high temperatures. Those gases potentially pollute the environment and damage the health of workers. High-fluorine mold fluxes also corrode casters as fluorine dissolves into the second-cooling water to form hydrofluoric acid[11,12].

Based on the disadvantages, efforts on developing low-fluorine and fluorine-free mold fluxes has been reported frequently. Mostly on $CaO-SiO_2-Na_2O$ and $CaO-SiO_2-TiO_2$ based systems[13-16]. However, industrial trials gave unstable performances of those fluorine-free or low-fluorine fluxes for peritectic steels, even their physical properties (melting temperature, viscosity, break temperature, and crystallization capacity etc.) are similar with conventional high-fluorine ones. Related research gives some possible explanations[17]: TiO_2-containing mold fluxes likely to deteriorate the lubrication capacity of liquid slag films and lead to a unstable casting(sticking or breakouts) because of the formation of titanium carbide and/or titanium carbonitride particles in molten fluxes (TiO_2 reacts with the carbon from sintering-control components and dissolved nitrogen in molten fluxes). Besides, the structure and evolution of the fluorine-decreased films during solidification (the roughness of surfaces in contacted with the mold, porosity, growth rate, and crystallization characteristics etc.) could be very different from conventional ones with

Peer-reviewed version available at Metals 2019, 9, 93; doi:10.3390/met9010093

a high-fluorine content, which also affect the performance of mold fluxes directly and are still unclear.

This study selected a typical low-fluorine $CaO-SiO_2-Na_2O$ based mold flux (which gives unstable performaces in commercial practices) and investigated the structure evolution of its films upon solidification. The structure differences were then, compared with conventional high-fluorine ones.

Previous approaches[18,19] used a water-cooled copper probe to solidify slag films from molten fluxes and obtain heat flux densities. However, some details of the previous probe are likely affected the results: First, the intensity cooling of the large probe surpasses the capacity of resistance furnaces to maintain a constant temperature of molten fluxes, which resulting a poor uniformity of film structures (especially the thickness and feature of the surface contacted with the probe). Second, the probe is in a cubic shape with small width-thickness ratio, the obtained solid films are more likely affected by two-dimension cooling, which could affect the structure of films. To solve those problems, a water-cooled copper probe with a much smaller volume and large width-thickness ratio was developed to obtain consistent film thicknesses, structures, and reliable heat flux densities [20, 24, 25].

2. Experimental method

2.1. Mold flux selection and slag film acquisition

A typical $CaO-SiO_2-Na_2O$ based low-fluorine (LF) mold flux was used as the basis of this study (see the composition in Table 1). Compared with conventional high-fluorine fluxes, this mold flux gave unstable performce in the casting of peritectic grade steels. Experimental samples were prepared using analytical-grade reagents ($CaCO_3$, SiO_2, Na_2CO_3, CaF_2 and Al_2O_3).

Preprints (www.preprints.org) | NOT PEER-REVIEWED | Posted: 6 December 2018 doi:10.20944/preprints201812.0079.v1

Peer-reviewed version available at Metals 2019, 9, 93; doi:10.3390/met9010093

The physical properties were measured[21-23] (see Table 2): The melting temperature was measured by the hemisphere point method; The high temperature viscosity and viscosity-temperature curve were measured by a high-temperature rotational viscometer (using graphite bobs with 15 mm diameter and graphite crucibles with 55mm inner diameter). The break temperature was defined as the temperature below which the flux viscosity increases sharply upon cooling at speed 6 K/min. For mold fluxes with a strong crystallization tendency, the break temperature approximately equal to the liquidus temperature.

Table 1. Composition of mold flux, mass percentages

CaO %/SiO_2 %	Al_2O_3	Na_2O	F
0.7	1	23	3

Table 2. Physical property of the mold flux

Viscosity$_{1300℃}$, Pa.s	Melting temperature, K	Break temperature, K
0.183	1431	1480

For each experiment, 300 g of pre-melted mold flux was loaded into a graphite crucible (60 mm inner diameter) and melted in a resistance furnace. The water-cooled probe was immersed into the melted flux to solidify slag films (probe size: 6 mm in thickness, 20 mm in length, 15mm in height; immersion depth: 13 mm; cooling water of the probe: 1.75 dm^3/ min). The heat flux densities through solid slag films were calculated using Equation 1, where Q is heat flux density, W is flow rate of cooling water, (T_{out} — T_{in}) is the temperature increase of water after which passes through the probe, A is the surface area that the probe contacted liquid fluxes, and C_p is the specific heat capacity of water. The solidified films were recovered after different probe immersion times (60 s, 90 s, and 120 s). Three slag bulk temperatures (1573 K, 1623 K, and 1673 K) were used to reveal the effect of bulk temperature on the structure and thermal property of solid films.

$$Q = \frac{W \cdot C_p (T_{out} - T_{in})}{1000 \cdot A} \quad (1)$$

Preprints (www.preprints.org) | NOT PEER-REVIEWED | Posted: 6 December 2018 doi:10.20944/preprints201812.0079.v1

Peer-reviewed version available at Metals 2019, 9, 93; doi:10.3390/met9010093

2.2. Measurements on solidified films

The thickness of solid films was measured with a point micrometer (six measurements for each wide-face film). The roughness of film surfaces in contacted with the copper probe was measured with a contact profilometer. The roughness (R_a) measurements were performed on the probe-side surface of each wide-face film (measuring six times). The illustrated positions, length, and direction of the roughness measurements are given in Figure 1a; The illustrated positions of thickness measurements are shown in Figure 1b.

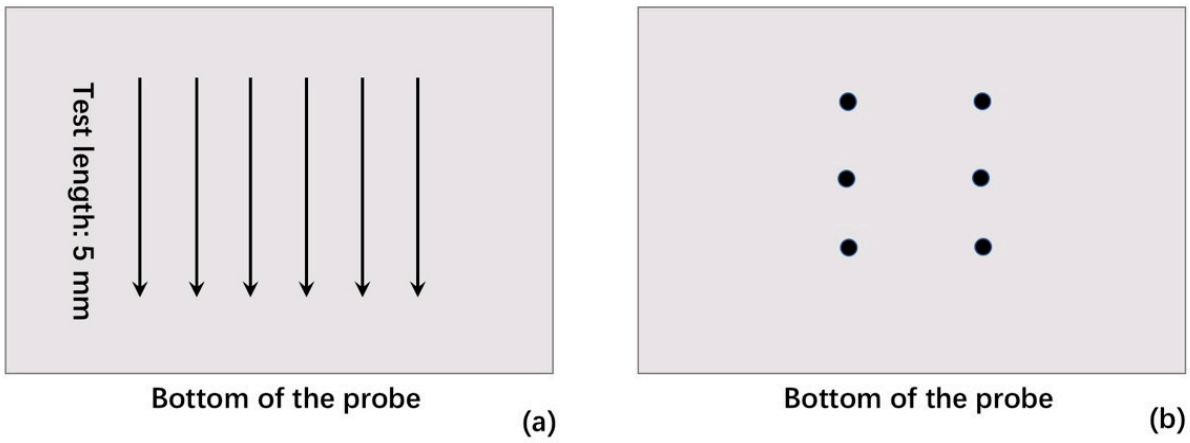

Figure 1. illustrated positions of surface roughness measurements (a) and thickness measurements (b). Films for measurement were recovered from the wide face of the probe.

The overall closed porosity of films was calculated. The apparent densities (d_a) of solid films and true densities (d_t, films pulverized into powders with size smaller than 45 μm) were measured by a gas pycnometry. The closed porosity of films can be calculated as $(d_t\text{-}d_a)/ d_t$.

Surface and internal features of films were inspected with scanning electron and optical microscopies. The cross-section samples were prepared after mounting films in resin and polishing with Al_2O_3 suspension. Samples for SEM were sputter coated with 2-3 nm of Pt. X-

Preprints (www.preprints.org) | NOT PEER-REVIEWED | Posted: 6 December 2018 doi:10.20944/preprints201812.0079.v1

Peer-reviewed version available at Metals 2019, 9, 93; doi:10.3390/met9010093

ray diffraction (Cu K_α radiation) was used to identify the major crystal of the pulverized film (the film sample recovered from molten flux with 1623K bulk temperature after 120 s immersion of the probe).

3. Results and discussions

3.1. Thickness and heat flux density of solid films

The results of the thickness and heat flux density of films are shown in Figure 2. As expected, the thickness of films increases gradually with decreased slag bulk temperatures and increased probe immersion times. Unstable heat flux densities are detected, especially at higher slag bulk temperature (1623K or 1673K) and short immersion time (within 20s, as marked with a rectangle in Figure 2). Besides intensive cooling, non-uniform cooling conditions at meniscuses also contribute to the formation of longitudinal cracks on initial steel shells. The unstable heat flux through low-fluorine films may contribute to its unstable performances. Other recent works show similar fluctuation of heat flux through solidified fluorine-free films[20], but for conventional and ultrahigh-basicity mold fluxes (with high F content), no apparent fluctuation was detected[24, 25]. The fluctuation of heat flux densities is partially contributed by the formation and evolution of internal cracks of glassy films upon solidification, which will be discussed below.

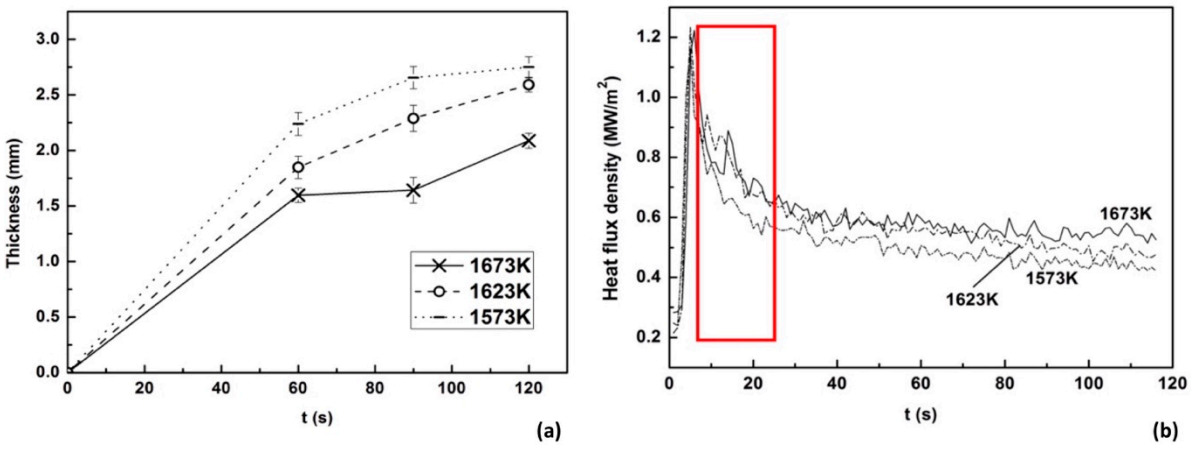

Figure 2. Thickness of solid films after different immersion times in molten fluxes with different bulk temperatures (a), error bars show standard deviations; and measured heat flux density (b).

3.2. Cracks formed in the glassy layer

Apparent internal cracks were observed (see Figure 3) in the glassy layer of solid films. Obvious fusion tendency of the crack boundaries indicates those cracks formed and fused during the immersion of probe in molten fluxes (not formed upon cooling after taking solidified films out of the molten flux). Intensive cooling of the water-cooled copper probe and the large temperature gradients of initial solidified films could cause the formation of cracks. The mechanism of the formation and evolution of those cracks is shown in Figure 4, which indicates the small pores with irregular shapes in the glass layer (see Figure 3a) are likely formed by the evolution(fusion) of cracks. As the formation of large cracks in the initial glassy film increases its thermal contact resistance (as Figure 4a and 4b show), the fusion of crack boundaries in contrast decreases the thermal contact resistance (Figure 4c). The continual formation and fusion of cracks naturally contributes to the heat flux fluctuation (especially in the early stage of solidification, as shown in Figure 2). No similar cracks and large heat flux fluctuations were observed in solid films with high ratio of crystals[20,24,25].

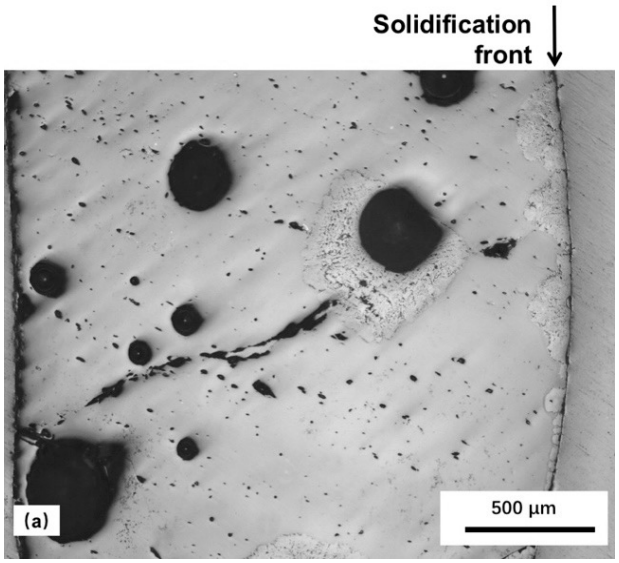

Preprints (www.preprints.org) | NOT PEER-REVIEWED | Posted: 6 December 2018 doi:10.20944/preprints201812.0079.v1

Peer-reviewed version available at Metals 2019, 9, 93; doi:10.3390/met9010093

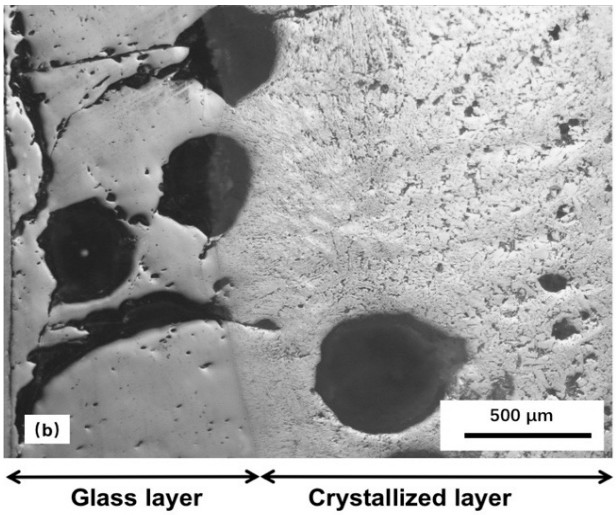

Figure 3. Cross-sections of films recovered from the molten flux with 1623K bulk temperature, after 60s (a) and 90s (b) of probe immersion; left of micrographs is the probe sides; crystals started to precipitate around the edge of pores in (a). (Optical micrographs, black regions and spots are pores and cracks)

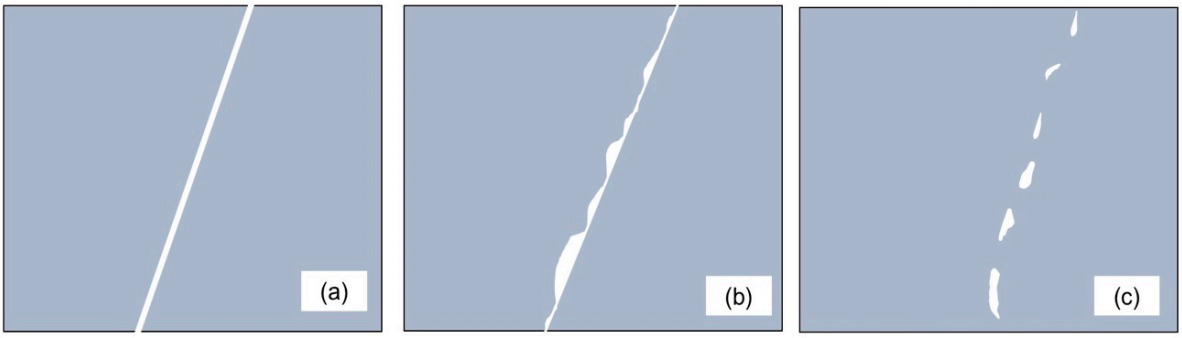

Figure 4. Schematic of the formation and evolution of cracks in the glassy layer (left of each graph refers to the probe sides): formation of initial cracks (a); the probe-side surface of the crack has a lower temperature (contributed by the interfacial thermal resistance of the crack) and larger shrinkage ratio upon cooling (b); some parts of the crack interface fuszed (molten flux side), isolated pores with irregular shapes formed (c); the white areas in (c) are pores.

Several recent researches suggest a film with higher basicity and cuspidine ratio tend to has a higher conductivity [26, 27]. The roughness of film surfaces contacted with the probe are with no causal relationship with crystallization[24, 25]. Although, those approaches indicate crystals contribute less on heat flux control directly, a low glass-ratio film is still expected to stabilize the heat flux within a micro zone: the worse performance of the low-fluorine mold flux in this work is likely partially caused by unstable heat fluxes through the slag films, because of the formation and fusion of internal cracks in the initial glassy films.

Peer-reviewed version available at Metals 2019, 9, 93; doi:10.3390/met9010093

Thus, besides the larger thermal contact resistance provided by the larger surface roughness of solid slag film, which already proved in other works[24, 25], another explanation of mold fluxes with high-basicity and high-fluorine content can provide more stable performaces than the mold flux applied in this study is: cracks form in a fully crystallized film does not have the evolution process as shown in Figure 4b and 4c, besides, a thicker film with a smaller ratio of glassy layer also decreases the effect of internal cracks on the heat flux fluctuations.

3.3. Surface roughness of solid films

The roughness of film surfaces in contacted with the copper wall increases the thermal contact resistance between steel shells and the mold, which is considered as one of the major contributions for heat flux control in continuous casting. The typical feature of film surfaces contacted with the probe is shown in Figure 6, and the measured roughness is given in Figure 5. The result indicates: for films obtained at higher bulk temperatures (1623K and 1673K), the difference of surface roughness is not statistically obvious when the immersion time less than 90 s, a longer probe immersion time gives lower roughness of films obtained at slag bulk temperature 1673K. The lower slag bulk temperature (1573 K) tends to result lower roughnesses. Some results demonstrate the formation of surface roughness for those films is not caused by crystallization or devitrification: the roughness did not increase with increased probe immersion times (even decreased continuously at slag bulk temperature 1673K). Figure 3a shows most part of the film cross section is glass, the surface contacted the probe is amorphous (the small particle with size around several micrometres detailed in Figure 6 is not crystals, which was confirmed by the microscopic analysis), but this film already has a very high roughness (as shown in Figure 5). Compared with the high-basicity and high-fluorine films[24, 25], the effect of bulk slag temperatures on roughness fluctuation is more obvious.

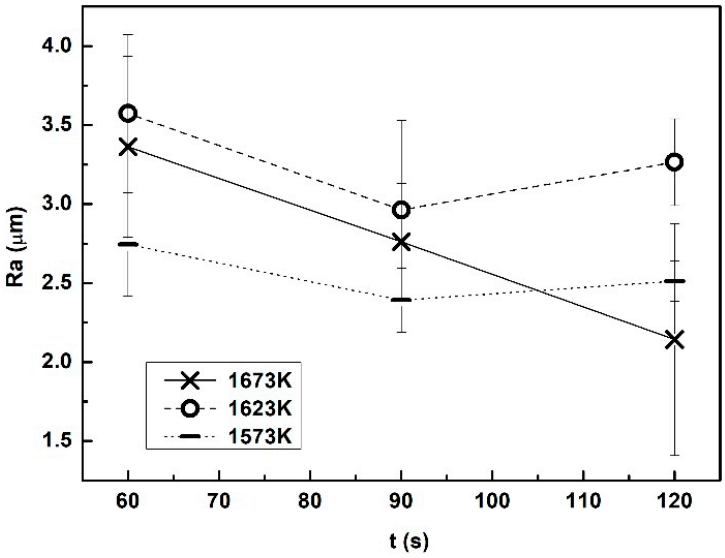

Figure 5. Roughness of film surfaces in contacted with the water-cooled copper probe, for films formed in molten flux with different bulk temperatures after different probe immersion times; error bars give the standard deviations.

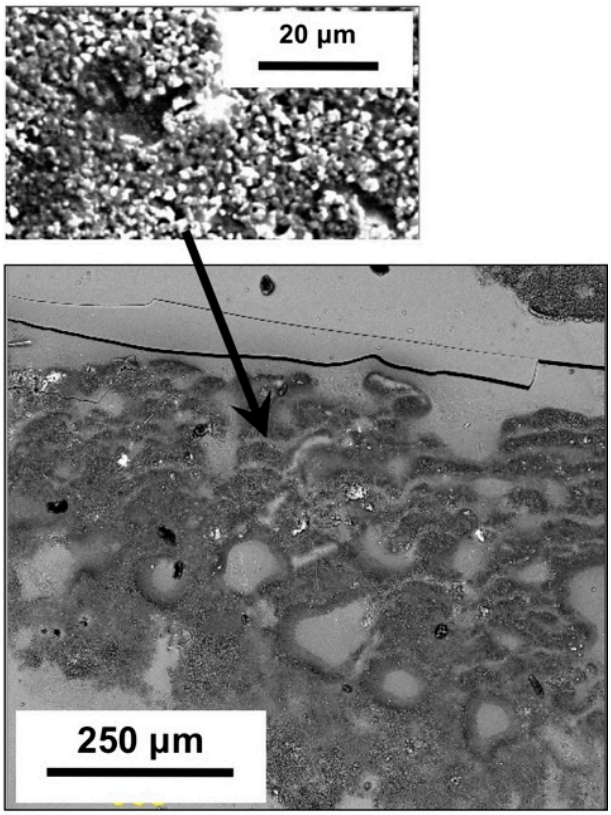

Figure 6. Appearance of the surface of a slag film in contacted with the probe; film recovered after 60s of immersion of the probe in 1623K mold flux (the film is almost glassy, secondary electron image).

3.4. Closed porosity and crystallization of films

Preprints (www.preprints.org) | NOT PEER-REVIEWED | Posted: 6 December 2018 doi:10.20944/preprints201812.0079.v1

Peer-reviewed version available at Metals 2019, 9, 93; doi:10.3390/met9010093

Closed pores in solid slag films decrease the effective thermal conductivity of films. The measured closed porosity of films is shown in Figure 7. The porosity tends to increase upon solidification. This result indicates pores also formed in the outer layer of solid films, which increase the overall porosity of films (especially for films obtained at 1623K, its porosity increased from about 2.17 to 8.40 volume percentage from 60 s to 120 s immersion of the probe). As to the relationship among the formation of pores and crystallization by solidification and devitrification, Figure 3 demonstrates: for this study, similar with high-fluorine mold fluxes [24, 25], before crystallization or devitrification, large pores were already existed in the glass films. Which indicates the formation of those large round-shape pores at the probe side of films has no causal relationship with crystallization or devitrification (although the devitrification may increase the porosity by forming micro-pores). The X-ray diffraction pattern in Figure 8 shows the major crystal in the film is combeite ($Ca_{1.543}Na_{2.914}Si_3O_9$) and those crystals are with columnar and faceted dendritic shapes (similar shape with conventional high-fluorine mold fluxes for peritectic steels, see Figure 9). Compared with conventional mold fluxes, this low-fluorine flux has a much lower crystallization and devitrification rate [24, 25].

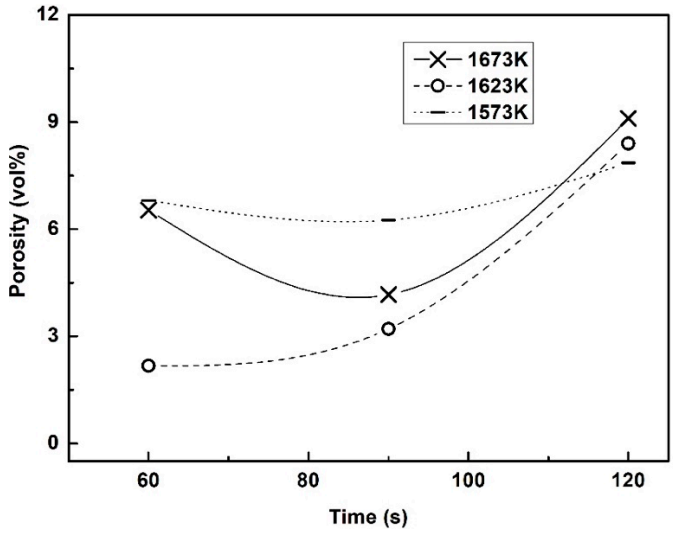

Figure 7. Closed porosity of films obtained at different slag bulk temperatures and probe immersion times.

Preprints (www.preprints.org) | NOT PEER-REVIEWED | Posted: 6 December 2018 doi:10.20944/preprints201812.0079.v1

Peer-reviewed version available at Metals 2019, 9, 93; doi:10.3390/met9010093

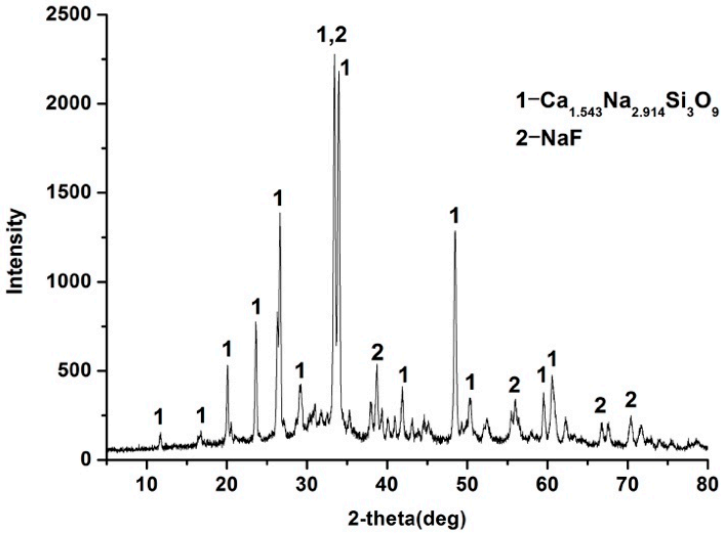

Figure 8. X-ray diffraction pattern of pulverized solid film (probe immersion time: 120s; slag temperature: 1623K; Cu K_α radiation).

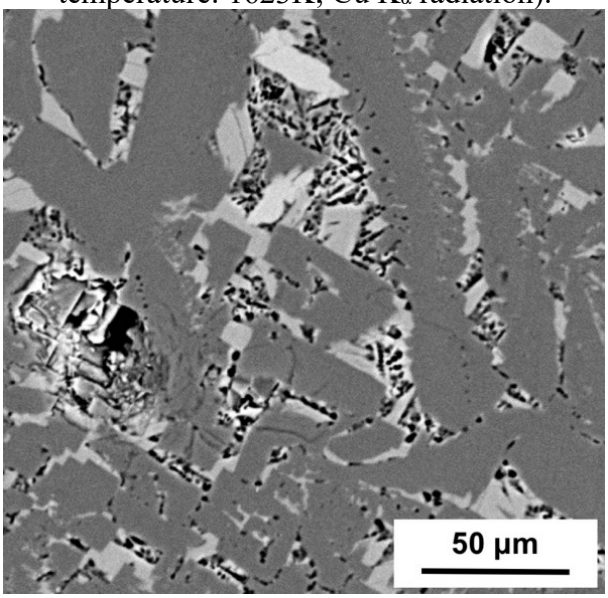

Figure 9. Typical micrograph of crystals in the solid film; the film was recovered after immersing the probe for 120s in molten flux with a bulk slag temperature 1623K. (backscattered electron image).

3.5. Density evolution of solidified films

To calculate the closed porosity of films, ture densites and apparent densities of slag films in solidification were measured accurately. The The density evolution of films was discussed as itself is an important feature of films. The apparent density and ture density of films are shown in Figure 10. Results show the temperature of liquid slag affects the density of solidified films directly. For the apparent density, films recovered from 1623 K flux give higher density values

Preprints (www.preprints.org) | NOT PEER-REVIEWED | Posted: 6 December 2018 doi:10.20944/preprints201812.0079.v1

Peer-reviewed version available at Metals 2019, 9, 93; doi:10.3390/met9010093

than ones recovered from the flux with other temperatures at short probe immersion times (60 and 90 s). Which partially caused by the difference of their closed porosity (see Figure 7). The temperature of molten flux and probe immersion time affect the true density of films obviously. As initial films are almost glass (proved by the cross-section morphology of films, such as Figure 3a), which has a relative low density, films recovered after 60 s of the probe immersion with different bulk temperatures give similar ture densities around 2.59 g/cm^3. When the immersion time reached 90 s, higher temperatures of molten fluxes result lower true densites of solidified films. As crystals of mold fluxes tend to have higher densities than the glass matrix has, the ture density change of solid film reflects the crystal ratio of films in solidification directly. The results indicate: for this mold flux, crystals begin to precipitate after 60 s of the probe immersion, for the probe immersion period 60 s to 90 s, a higher bulk temperature results a relative lower crystallization rate and ratio. Which related to the larger temperature gradient of films solidified in high temperature molten fluxes, because crystallization needs sufficient supercooling at the solidification front. However, in the probe immersion period 90 s to 120 s, the crystallization rate of films solidified in the higher temperature flux increases obviously. Which caused by a faster devitrification rate in the glassy film at the probe side (higher bulk tempertuare gives larger temperature gradient and also increases the temperature of the probe-side part of films for divitrification).

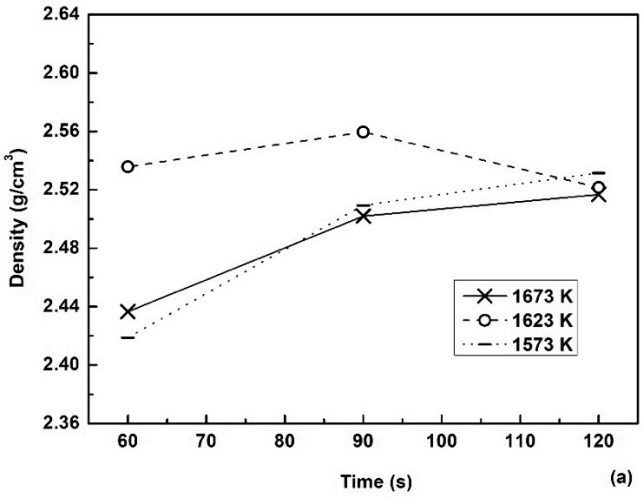

Preprints (www.preprints.org) | NOT PEER-REVIEWED | Posted: 6 December 2018 doi:10.20944/preprints201812.0079.v1

Peer-reviewed version available at Metals 2019, 9, 93; doi:10.3390/met9010093

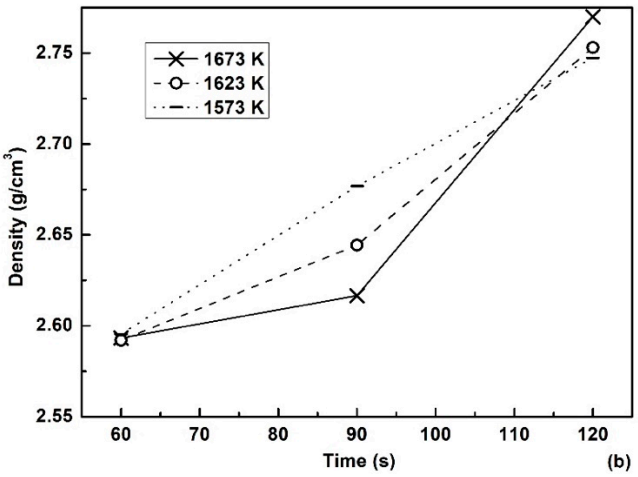

Figure 10. Apparent densities(a) and true densities (b) of slag films obtained at different slag bulk temperatures and probe immersion times.

4. Conclusions

In this study, a low-fluorine mold flux was solidified by an improved water-cooled copper probe. The heat flux through solid films was calculated and film samples were recovered and inspected. Based on the results, some conclusions can be drawn:

(1) Internal cracks in initial solidified glassy films were observed, the formation and fusion of those cracks during solidification are likely contributed to the fluctuation of heat flux density, especially at the early stage of film solidification.

(2) The roughness of surfaces in contacted with the water-cooled probe formed early before crystallization or devitrification, and which is obviously affect by the temperature of molten fluxes and probe immersion time. The formation of closed pores in the probe-side glassy films has no causal relationship with crystallization.

(3) Combeite($Ca_{1.543}Na_{2.914}Si_3O_9$) with columnar and faceted dendritic shapes is the major crystal in solid films.

Acknowledgements

The authors would like to appreciate the support from Natural Science Foundation of China (project No. 51874057 and U1660204). Professor P. C. Pistorius of Carnegie Mellon University

is deeply appreciated for the valuable discussion and guidance on the improved water-cooled copper probe device.

References

[1] H. Nakada, M. Susa, Y. Seko, M. Hayashi, and K. Nagata. Mechanism of Heat Transfer Reduction by Crystallization of Mold Flux for Continuous Casting. *ISIJ Int.*, 2008, 48, 446-53.

[2] A. Yamauchi, K. Sorimachi, T. Sakuraya, and T. Fujii. Heat Transfer between Mold and Strand through Mold Flux Film in Continuous Casting of Steel. *ISIJ Int.*, 1993, 33, 140-47.

[3] K. C. Mills, and A. B. Fox. The Role of Mould Fluxes in Continuous Casting-So Simple Yet So Complex. *ISIJ Int*., 2003, 43, 1479-86.

[4] K. C. Mills, A. B. Fox, Z. Li, and R. P. Thackray. Proc. VII Int. Conf on Molten Slags, Fluxes and Salts, The South African Institute of Mining and Metallurgy, Cape Town, South Africa, 2004.

[5] J. Brimacombe and K. Sorimachi. Crack formation in the continuous casting of steel. *Metall. Trans. B*, 1977, 8B, 489-505.

[6] G. H. Wen, S. Sridhar, P. Tang, X. Qi, and Y. Q. Liu. Development of fluoride-free mold powders for peritectic steel slab casting. *ISIJ Int.*, 2007, 47, 1117-25.

[7] A. Fox, K. Mills, D. Lever, C. Bezerra, C. Valadares, I. Unamuno, J. Laraudogoitia, and J. Gisby. Development of Fluoride-Free Fluxes for Billet Casting. *ISIJ Int.*, 2005, 45, 1051-58.

[8] H. Nakada, H. Fukuyama, K. Nagata. Effect of NaF Addition to Mold Flux on Cuspidine Primary Field. *ISIJ Int.*, 2006, 46, 1660-67.

[9] H. Nakada, K. Nagata. Crystallization of $CaO–SiO_2–TiO_2$ slag as a candidate for fluorine free mold flux. *ISIJ Int.*, 2006, 46, 441-449.

[10] J. W. Cho, T. Emi, H. Shibata and M. Suzuki. Heat transfer across mold flux film in mold during initial solidification in continuous casting of steel. *ISIJ Int.*, 1998, 38, 834-42.

[11] M. D. Seo, C. B. Shi, J. W. Cho, S. H. Kim. Crystallization behaviors of CaO-SiO_2-Al_2O_3-Na_2O-CaF_2-(Li_2O-B_2O_3) mold fluxes. *Metall. Mater. Trans. B,* 2014, 45, 1874-86.

[12] M. Persson, S. Sridhar, S. Seetharaman. Kinetic Studies of Fluoride Evaporation from Slags. *ISIJ Int.*, 2007, 47, 1711-17.

[13] Z. Wang, Q. Shu, K. Chou. Viscosity of Fluoride-Free Mold Fluxes Containing B_2O_3 and TiO_2, *Steel Res. Int.,* 2013, 84, 766-76.

[14] G. Fan, S. He, T. Wu, and Q. Wang. Effect of Fluorine on the Structure of High Al_2O_3-Bearing System by Molecular Dynamics Simulation. *Metall. Mater. Trans. B*, 2015, 46, 2005-13.

[15] B. Lu, W. Wang. Effects of Fluorine and BaO on the Crystallization Behavior of Lime–Alumina-Based Mold Flux for Casting High-Al Steels. *Metall. Mater. Trans. B*, 2015, 46, 852-62.

[16] S. He, Q. Wang, D. Xie, C. Xu, Z. S. Li, K. C. Mills. Solidification and crystallization properties of CaO-SiO2-Na2O based mold fluxes. *Int. J. Min. Metall. Mater.*, 2009, 16, 261-64.

[17] Q. Wang, Y. Lu, S. He, K. Mills, Z. S. Li. Formation of TiN and Ti (C, N) in TiO_2 containing, fluoride free, mould fluxes at high temperature. *Ironmak. Steelmak.,* 2011, 38, 297-301.

[18] G. Wen, S. Sridhar, P. Tang, X. Qi and Y. Liu. Development of fluoride-free mold powders for peritectic steel slab casting. *ISIJ Int.*, 2007, 47, 1117-25.

[19] H. Ryu, Z. Zhang, J. W. Cho. G. Wen and S. Sridhar. Crystallization behaviors of slags through a heat flux simulator. *ISIJ Int.*, 2010, 50, 1142-50.

[20] K. Lara Santos Assis. Heat transfer through mold fluxes: a new approach to measure thermal properties of slags, *Ph.D. Thesis*, Carnegie Mellon University, Pittsburgh, Feb. 2016.

[21] X. Long, S. He, J. Xu, X. Huo, and Q. Wang. Properties of high basicity mold fluxes for peritectic steel slab casting. *J. Iron Steel Res. Int.*, 2012, 19, No. 7, 39-45.

[22] S. He, X. Long, J. Xu, T. Wu, and Q. Wang. Effects of crystallisation behaviour of mould fluxes on properties of liquid slag film. *Ironmak. Steelmak.,* 2012, 39, 593-98.

[23] T. Wu, Q. Wang, S. He, J. Xu, X. Long, and Y. Lu. Study on properties of alumina-based mould fluxes for high-Al steel slab casting. *Steel Res. Int.,*2012, 83, 1194-1202.

[24] X. Long, Q. Wang, S. He, and P. C. Pistorius. Structure evolution of slag films of ultrahigh-basicity mold flux during solidification. *Metall and Materi Trans B*, 2017, 48, 1938-42.

[25] X. Long, S. He, Q. Wang and P. C. Pistorius. Structure of solidified films of mold flux for peritectic steel. *Metall and Materi Trans B*, 2017, vol 48, 1652-58.

[26] J. A. Kromhout, E. R. Dekker, M. Kawamoto, and R. Boom. Challenge to control mould heat transfer during thin slab casting. *Ironmak. Steelmak*., 2013, 40, 206-215.

[27] S. P. Andersson and C. Eggertson. Thermal conductivity of powders used in continuous casting of steel, part 1 – glassy and crystalline slags. *Ironmak. Steelmak.*, 2015, 42, 456-64.

Peer-reviewed version available at Metals 2019, 9, 93; doi:10.3390/met9010093

Figure captions:

Figure 1. illustrated positions of surface roughness measurements (a) and thickness measurements (b). Films for measurement were recovered from the wide face of the probe.

Figure 2. Thickness of solid films after different immersion times in molten fluxes with different bulk temperatures (left, error bars show standard deviations); measured heat flux density (at right).

Figure 3. Cross-sections of films recovered from the molten flux with 1623K bulk temperature, after 60s (a) and 90s (b) of probe immersion; left of micrographs is the probe sides; crystals started to precipitate around the edge of pores in (a). (Optical micrographs, black regions and spots are pores and cracks)

Figure 4. Schematic of the formation and evolution of cracks in the glassy layer (left of each graph refers to the probe sides): formation of initial cracks (a); the probe-side surface of the crack has a lower temperature (contributed by the interfacial thermal resistance of the crack) and larger shrinkage ratio upon cooling (b); some parts of the crack interface fuszed, isolated pores with irregular shapes formed (c); the white areas in (c) are pores.

Figure 5. Roughness of film surfaces in contacted with the water-cooled copper probe, for films formed in molten flux with different bulk temperatures after different probe immersion times; error bars give the standard deviations.

Figure 6. Appearance of the surface of a slag film in contacted with the probe; film recovered after 60s of immersion of the probe in 1623K mold flux (the film is almost glassy, secondary electron image).

Figure 7. Closed porosity of films obtained at different slag bulk temperatures and probe immersion times.

Figure 8. X-ray diffraction pattern of pulverized solid film (probe immersion time: 120s; slag temperature: 1623K; Cu K_{α} radiation).

Figure 9. Typical micrograph of crystals in the solid film; the film was recovered after immersing the probe for 120s in molten flux with a bulk slag temperature 1623K. (backscattered electron image).

Figure 10. Apparent densities(a) and true densities (b) of slag films obtained at different slag bulk temperatures and probe immersion times.

Tables:

Table 1. Composition of mold flux, mass percentages

CaO %/SiO_2 %	Al_2O_3	Na_2O	F
0.7	1	23	3

Table 2. Physical property of the mold flux

Viscosity$_{1300℃}$, Pa.s	Melting temperature, K	Break temperature, K
0.183	1431	1480